11. Rea D, Nicolini FE, Tulliez M, et al; France Intergroupe des Leucémies Myéloïdes Chroniques. Discontinuation of dasatinib or nilotinib in chronic myeloid leukemia: interim analysis of the STOP 2G-TKI study. *Blood*. 2017; 129(7):846-854.

12. Hochhaus A, Masszi T, Giles FJ, et al. Treatment-free remission following frontline nilotinib in patients with chronic myeloid leukemia in chronic phase: results from the ENESTfreedom study. *Leukemia*. 2017;31(7):1525-1531.

13. Branford S, Yeung DT, Parker WT, et al. Prognosis for patients with CML and >10% BCR-ABL1 after 3 months of imatinib depends on the rate of BCR-ABL1 decline. *Blood*. 2014;124(4):511-518.

DOI 10.1182/blood.2019000120

TO THE EDITOR:

A population of CD20$^+$CD27$^+$CD43$^+$CD38$^{lo/int}$ B1 cells in PNH are missing GPI-anchored proteins and harbor *PIGA* mutations

Yuki Kageyama,[1] Hiroshi Miwa,[1] Isao Tawara,[1] Kohshi Ohishi,[2] Masahiro Masuya,[1] and Naoyuki Katayama[1]

[1]Department of Hematology and Oncology, Mie University Graduate School of Medicine, Tsu, Japan; and [2]Department of Transfusion Medicine and Cell Therapy, Mie University Hospital, Tsu, Japan

B1 cells were first described in 1983 as a rare B-lymphocyte subpopulation that spontaneously secreted immunoglobulin M (IgM) and appeared to be distinguished from B2 cells.[1] The functional properties, phenotype, and ontogeny of B1 cells differ from those of B2 cells.[2] In mice, B1 cells emerge independently of hematopoietic stem cells (HSCs) during early embryonic development[3,4] and are then produced by HSCs or HSC-derived progenitors in the fetal liver and in neonatal and adult bone marrow,[5] whereas B2 cells are generated from HSCs. In contrast to murine B1 cells, the characteristics of human B1 cells had not been well understood. In 2011, it was reported that human B1 cells have the phenotype CD20$^+$CD27$^+$CD43$^+$CD70$^-$.[6] However, these cells were later found to include CD20$^+$CD38^{hi} precursors to plasmablasts or preplasmablasts.[7,8] Consequently, CD20$^+$CD27$^+$CD43$^+$CD38$^{lo/int}$ is currently regarded as a more accurate phenotype of human B1 cells.[8] B1 cells are detected in adult human peripheral blood (PB) at a frequency of between 1% and 9% of B cells.[6,9,10] However, the developmental origin of human B1 cells remains elusive.

To elucidate whether human B1 cells are derived from adult HSCs, we used a unique characteristic of patients with paroxysmal nocturnal hemoglobinuria (PNH), a clonal disorder of HSCs caused by somatic mutations in *PIGA* that encodes the protein essential for glycophosphatidylinositol (GPI)-anchor biosynthesis.[11-13] Importantly, the *PIGA*-mutated HSCs retain

Table 1. Characteristics of PNH patients

Patient	Sex	Sampling time point	Age at sampling, y	Time after diagnosis, y	WBC, ×10^9/L	Hb, g/dL	Platelets, ×10^9/L	LDH, IU/L*	Treatment at sampling
PNH01	Female	First	44	20	2.4	9.3	101	274	Eculizumab
		Second†	46	22	5.3	9.6	142	192	Eculizumab
PNH02	Female	First	54	28	3.8	11.9	194	195	Eculizumab
		Second‡	57	31	3.3	11.5	119	205	Eculizumab
PNH03	Female	First	83	15	1.6	10.4	107	208	Eculizumab
		Second§	86	18	1.5	9.8	111	215	Eculizumab
PNH04	Female	First	63	3	6.3	7.1	41	168	Cyclosporin A; eculizumab
PNH05	Female	First	49	5	3.7	6.8	180	1898	Metenolone; RBC transfusion
PNH06	Female	First	28	3	5.5	10.6	191	670	Cyclosporin A

Hb, hemoglobin; LDH, lactate dehydrogenase; RBC, red blood cell; WBC, white blood cell.

*Normal range, 110 to 225 IU/L.

†After 24 months from first sampling.

‡After 29 months from first sampling.

§After 35 months from first sampling.

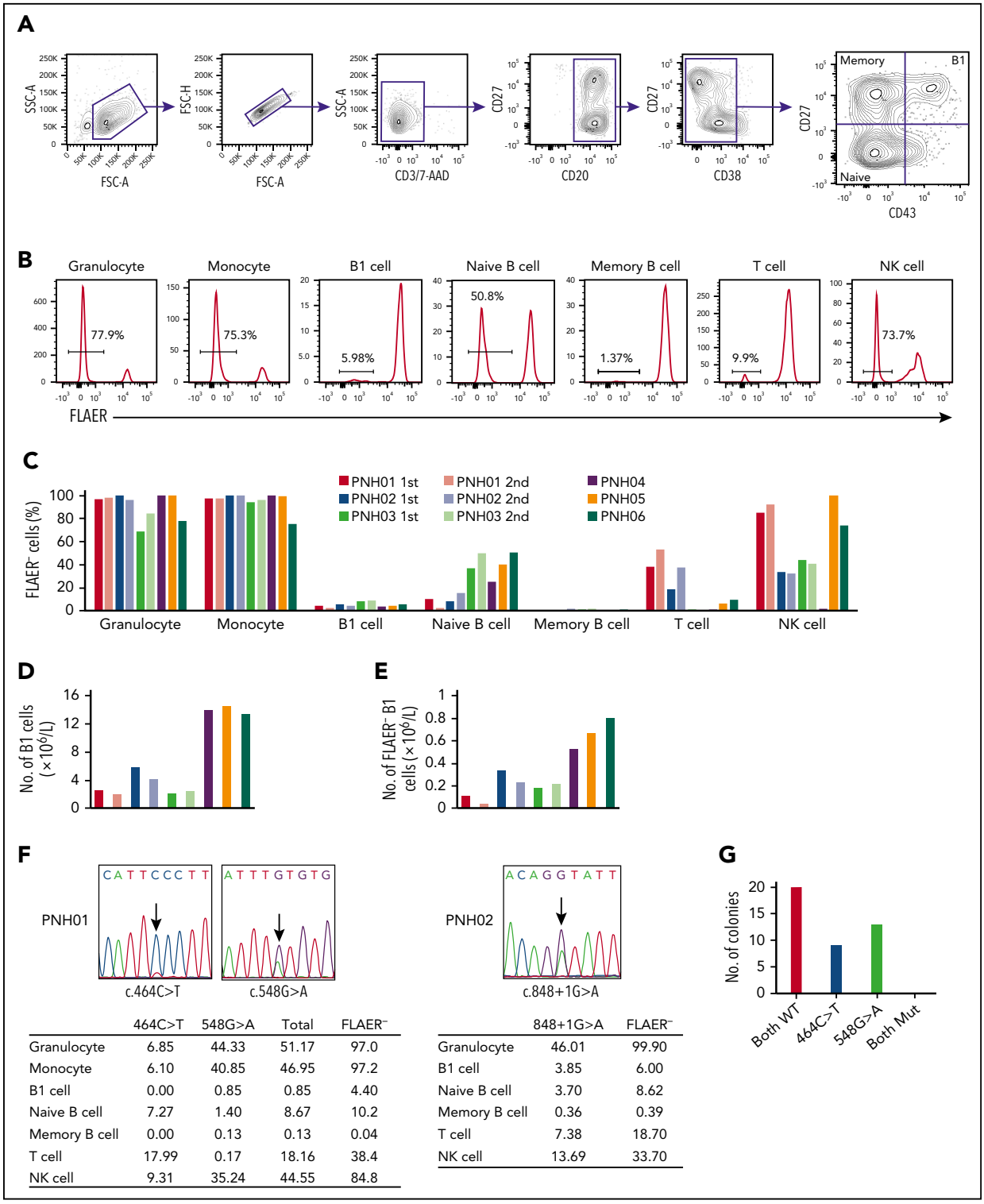

	464C>T	548G>A	Total	FLAER⁻
Granulocyte	6.85	44.33	51.17	97.0
Monocyte	6.10	40.85	46.95	97.2
B1 cell	0.00	0.85	0.85	4.40
Naive B cell	7.27	1.40	8.67	10.2
Memory B cell	0.00	0.13	0.13	0.04
T cell	17.99	0.17	18.16	38.4
NK cell	9.31	35.24	44.55	84.8

	848+1G>A	FLAER⁻
Granulocyte	46.01	99.90
B1 cell	3.85	6.00
Naive B cell	3.70	8.62
Memory B cell	0.36	0.39
T cell	7.38	18.70
NK cell	13.69	33.70

Figure 1. GPI-AP deficiency and *PIGA* mutations in each cell population of PB from PNH patients. (A) Gating strategy to analyze and sort B1 cells and other B-lineage cells from PNH patients. CD19 cells were enriched using microbeads and gated as shown. Doublets were excluded based on forward scatter (FSC) profiles, and dead cells and T cells were excluded by gating 7-aminoactinomycin D–negative (7-AAD$^-$) and CD3$^-$ cells, respectively. B-cell subsets were defined as: B1 cells, CD19$^+$CD20$^+$CD27$^+$CD43$^+$CD38$^{lo/int}$; naive B cells, CD19$^+$CD20$^+$CD27$^-$CD43$^-$CD38$^{lo/int}$; and memory B cells, CD19$^+$CD20$^+$CD27$^+$CD43$^-$CD38$^{lo/int}$. (B) Representative histograms of FLAER staining in granulocytes, monocytes, B1 cells, naive B cells, memory B cells, T cells, and natural killer (NK) cells from PNH06. Percentages indicate FLAER$^-$ cells. (C) Percentages of FLAER$^-$ cells in the indicated PB-cell populations in the first and second samples from the 6 PNH patients. Second samples were obtained from PNH01, PNH02, and PNH03. (D) Absolute numbers of B1 cells. The absolute numbers of B1 cells were calculated by multiplying the number of CD19$^+$ cells by the percentage of B1 cells in CD19$^+$ cells (supplemental Table 4). (E) Absolute numbers of FLAER$^-$ B1 cells. The absolute numbers of FLAER$^-$ B1 cells were calculated by multiplying the number of B1 cells by the percentage of FLAER$^-$ B1 cells (supplemental Table 4). (F) Sanger sequences of the *PIGA* gene indicating the 2 mutations in PNH01 and 1 mutation in PNH02. The tables below show the percentages of the *PIGA*-mutated allele frequencies in each cell population measured by digital PCR. (G) Results of sequencing of bacterial colonies transfected with plasmids carrying genomic DNA from PNH01. FSC-A, FSC–area; FSC-H, FSC–height; Mut, mutated; SSC-A, side scatter–area; WT, wild type.

their multilineage differentiation capacity, and these mutations can be exploited to identify cells derived from adult HSCs. Because *PIGA* mutations abolish cell-surface GPI-anchored proteins (GPI-APs), we separated the mutated cells by the absence of GPI-APs.[14]

We enrolled 6 patients with a median time from PNH diagnosis of 10 years (range, 3-28 years; Table 1). PB samples were obtained from these PNH patients (who gave written informed consent) and stored at the Mie University Biobank Research Center. The study design was approved by the Independent Ethics Committee for Human Research at Mie University Graduate School of Medicine and was conducted in accordance with the Declaration of Helsinki. At the time of the first or second sampling, 3 patients were being treated with eculizumab alone, 1 with eculizumab and cyclosporin A, 1 with metenolone and red blood cell transfusion, and 1 with cyclosporin A alone.[12,15] Isolated PB cells were stained with fluorochrome-conjugated monoclonal antibodies (supplemental Table 1, available on the *Blood* Web site). Because fluorescent-labeled inactive toxin aerolysin (FLAER; Cedarlane, Burlington, ON, Canada) specifically and strongly binds to all cell-surface GPI-APs, FLAER was used to detect GPI-AP–deficient cells. Samples were analyzed and sorted into each cell population. Genomic DNA was extracted from sorted cells. The exons of the *PIGA*-coding region were amplified by polymerase chain reaction (PCR), and the products were sequenced. Allelic frequencies of *PIGA* mutations of genomic DNA from patients PNH01 and PNH02 were estimated by digital PCR (supplemental Table 2). Genomic DNA of PNH01 was amplified using PCR primers covering the 2 mutation sites and was used for sequencing. Further details of the experimental procedures are provided in the supplemental Materials and methods.

Granulocytes and monocytes were identified by CD45 and side scatter, and confirmed to be $CD11b^{hi}$ and $CD33^{hi}$, respectively. B-cell subpopulations were defined as follows: B1 cells, $CD19^+CD20^+CD27^+CD43^+CD38^{lo/int}$; naive B cells, $CD19^+CD20^+CD27^-CD43^-CD38^{lo/int}$; and memory B cells, $CD19^+CD20^+CD27^+CD43^-CD38^{lo/int}$ (Figure 1A). T cells and natural killer (NK) cells were identified as $CD3^+CD19^-CD33^-$ and $CD3^-CD19^-CD33^-CD56^+$, respectively. GPI-AP–deficient cells were identified as being $FLAER^-$ cells (Figure 1B).[16] The proportion of $FLAER^-$ PNH cells in each cell population varied among the first samples taken from all 6 patients, consistent with previous reports.[17-19] Granulocytes and monocytes had the highest proportions of $FLAER^-$ cells in all 6 patients (ranges, 68.5% to 100% and 75.3% to 100%, respectively; Figure 1C; supplemental Table 3). The absolute number of B1 cells varied among the samples and ranged from 2.17×10^6/L to 14.52×10^6/L (Figure 1D; supplemental Table 4). All 6 samples analyzed contained PNH phenotype cells in the B1 cell fraction (ranges, 3.79% to 8.39% and 0.11×10^6/L to 0.80×10^6/L; Figure 1C,E; supplemental Tables 3 and 4). Potential explanations for the low proportion of $FLAER^-$ B1 cells are not obvious. Approximately 50% of $FLAER^-$ B1 cells from patients PNH02 and PNH03 expressed IgM and IgD (supplemental Figure 1), compatible with the proposal by Rothstein et al.[20] These data indicate that a population of B1 cells is derived from *PIGA*-mutated HSCs. The frequency of B1 cells did not differ significantly between $FLAER^-$ and $FLAER^+$ cells in the $CD19^+CD20^+CD38^{lo/int}$ cell population (supplemental Figure 2). It seems unlikely that GPI-AP deficiency could influence the development of B1 cells. The second analyses in patients PNH01, PNH02, and PNH03 at the 24-, 29-, and 35-month intervals, respectively, again showed variability in the proportion of $FLAER^-$ cells in each cell population (Figure 1C,E; supplemental Table 3). Whereas a certain amount of $FLAER^-$ naive B cells was observed in all samples (range, 2.73% to 50.8%), the fraction of $FLAER^-$ memory B cells was extremely small (range, 0.04% to 1.96%). It is possible that GPI-AP deficiency might affect the formation and/or maintenance of memory B cells. Another possibility is that nearly all $FLAER^-$ memory B cells are generated before the onset of PNH and have a long lifespan.

Two *PIGA* mutations (c.464C>T and c.548G>A) were identified in PNH01 (Figure 1F). Follow-up bacterial cloning analysis demonstrated that the mutations were not present in the same clones (Figure 1G). A single *PIGA* mutation (c.848+1G>A) was identified in PNH02 (Figure 1F). We sorted each leukocyte subpopulation and measured the mutated allelic frequency by digital PCR with mutation-specific TaqMan probes. Because patients PNH01 and PNH02 were both female, 1 of the 2 X chromosomes, where the *PIGA* gene is located, is inactivated and a *PIGA* mutation in 1 allele renders cells negative for FLAER. This fact is compatible with our finding that the percentage of cells with *PIGA* gene mutations in each cell population was approximately one-half that of the $FLAER^-$ cells detected by flow cytometry (Figure 1F). Notably, the same mutations detected in B1 cells were also observed in other cell lineages.

Two experimental strategies have been used to examine the origin of B1 cells, namely xenotransplantation and gene-labeling assays. Quách et al recently reported that HSCs from adult human bone marrow and human cord blood produce B1 cells after transplantation into immunodeficient mice.[21] However, it is possible that a small amount of B1 cells or their progenitors was included among the transplanted cells. In the second approach, Sawai et al designed an HSC-selective inducible lineage-tracing technique in mice and found that <5% of B1 cells were labeled, compared with >50% of conventional B2 cells.[22] Because a comparable experiment cannot be conducted in humans, we took advantage of the naturally occurring clonal mutations present in PNH patients, which allowed us to analyze unmanipulated PB cells. Using such a strategy, Corat et al reported the existence of a long-lived, adaptive NK-cell population.[23]

The present study shows that a population of B1 cells in PNH patients is deficient for GPI-APs and carries *PIGA* mutation(s). These results offer the possibility that a small, but distinct, proportion of B1 cells may be derived from adult HSCs, although they were obtained from an investigation conducted in diseased patients.

Acknowledgments

The authors thank all clinicians who contributed materials, particularly A. Sawaki (Yokkaichi Municipal Hospital), T. Yamaguchi (Suzuka Chuo General Hospital), and Y. Uemura (Saiseikai Matsusaka General Hospital). The authors acknowledge the Mie University Biobank Research Center for sample preservation and the Mie University Center for Molecular Biology and Genetics for technical assistance. The authors thank Anne M. O'Rourke, Mitchell Arico, and Michelle Kahmeyer-Gabbe from Edanz Group (www.edanzediting.com/ac) for editing a draft of this manuscript.

This work was supported by the Japan Society for the Promotion of Science Grants-in-Aid for Scientific Research (KAKENHI grant numbers 17K099230, 16K093070, and 17K099490).

Authorship

Contribution: Y.K., H.M., and N.K. designed the study; Y.K. performed the experiments, analyzed the data, and created the figures; Y.K., H.M., I.T., K.O., and M.M. analyzed the data; Y.K and H.M. wrote the manuscript; N.K. reviewed and edited the manuscript; and all authors approved the final version of the manuscript.

Conflict-of-interest disclosure: The authors declare no competing financial interests.

ORCID profiles: Y.K., 0000-0002-0564-2227; I.T., 0000-0002-5426-9422.

Correspondence: Naoyuki Katayama, Department of Hematology and Oncology, Mie University Graduate School of Medicine, 2-174 Edobashi, Tsu, Mie 514-8507, Japan; e-mail: n-kata@clin.medic.mie-u.ac.jp.

Footnotes

For original data, please contact n-kata@clin.medic.mieu. ac.jp.

The online version of this article contains a data supplement.

REFERENCES

1. Hayakawa K, Hardy RR, Parks DR, Herzenberg LA. The "Ly-1 B" cell subpopulation in normal immunodefective, and autoimmune mice. *J Exp Med*. 1983;157(1):202-218.
2. Hayakawa K, Hardy RR, Herzenberg LA, Herzenberg LA. Progenitors for Ly-1 B cells are distinct from progenitors for other B cells. *J Exp Med*. 1985;161(6):1554-1568.
3. Yoshimoto M, Montecino-Rodriguez E, Ferkowicz MJ, et al. Embryonic day 9 yolk sac and intra-embryonic hemogenic endothelium independently generate a B-1 and marginal zone progenitor lacking B-2 potential. *Proc Natl Acad Sci USA*. 2011;108(4):1468-1473.
4. Kobayashi M, Shelley WC, Seo W, et al. Functional B-1 progenitor cells are present in the hematopoietic stem cell-deficient embryo and depend on Cbfβ for their development. *Proc Natl Acad Sci USA*. 2014;111(33):12151-12156.
5. Montecino-Rodriguez E, Dorshkind K. B-1 B cell development in the fetus and adult. *Immunity*. 2012;36(1):13-21.
6. Griffin DO, Holodick NE, Rothstein TL. Human B1 cells in umbilical cord and adult peripheral blood express the novel phenotype CD20+ CD27+ CD43+ CD70- [published corrections appear in *J Exp Med*. 2011;208(2):409 and *J Exp Med*. 2011;208(4):871]. *J Exp Med*. 2011;208(1):67-80.
7. Covens K, Verbinnen B, Geukens N, et al. Characterization of proposed human B-1 cells reveals pre-plasmablast phenotype. *Blood*. 2013;121(26):5176-5183.
8. Quách TD, Rodríguez-Zhurbenko N, Hopkins TJ, et al. Distinctions among circulating antibody-secreting cell populations, including B-1 cells, in human adult peripheral blood. *J Immunol*. 2016;196(3):1060-1069.
9. Descatoire M, Weill JC, Reynaud CA, Weller S. A human equivalent of mouse B-1 cells? *J Exp Med*. 2011;208(13):2563-2564.
10. Perez-Andres M, Grosserichter-Wagener C, Teodosio C, van Dongen JJ, Orfao A, van Zelm MC. The nature of circulating CD27+CD43+ B cells. *J Exp Med*. 2011;208(13):2565-2566.
11. Terstappen LW, Nguyen M, Huang S, Lazarus HM, Medof ME. Defective and normal haematopoietic stem cells in paroxysmal nocturnal haemoglobinuria. *Br J Haematol*. 1993;84(3):504-514.
12. Brodsky RA. Paroxysmal nocturnal hemoglobinuria. *Blood*. 2014;124(18):2804-2811.
13. Maciejewski JP, Sloand EM, Sato T, Anderson S, Young NS. Impaired hematopoiesis in paroxysmal nocturnal hemoglobinuria/aplastic anemia is not associated with a selective proliferative defect in the glycosylphosphatidylinositol-anchored protein-deficient clone. *Blood*. 1997;89(4):1173-1181.
14. Takeda J, Miyata T, Kawagoe K, et al. Deficiency of the GPI anchor caused by a somatic mutation of the PIG-A gene in paroxysmal nocturnal hemoglobinuria. *Cell*. 1993;73(4):703-711.
15. Hillmen P, Hall C, Marsh JC, et al. Effect of eculizumab on hemolysis and transfusion requirements in patients with paroxysmal nocturnal hemoglobinuria. *N Engl J Med*. 2004;350(6):552-559.
16. Borowitz MJ, Craig FE, Digiuseppe JA, et al; Clinical Cytometry Society. Guidelines for the diagnosis and monitoring of paroxysmal nocturnal hemoglobinuria and related disorders by flow cytometry. *Cytometry B Clin Cytom*. 2010;78(4):211-230.
17. Richards SJ, Morgan GJ, Hillmen P. Immunophenotypic analysis of B cells in PNH: insights into the generation of circulating naive and memory B cells. *Blood*. 2000;96(10):3522-3528.
18. Cui W, Fan Y, Yang M, Zhang Z. Expression of CD59 on lymphocyte and the subsets and its potential clinical application for paroxysmal nocturnal hemoglobinuria diagnosis. *Clin Lab Haematol*. 2004;26(2):95-100.
19. Katagiri T, Kawamoto H, Nakakuki T, et al. Individual hematopoietic stem cells in human bone marrow of patients with aplastic anemia or myelodysplastic syndrome stably give rise to limited cell lineages. *Stem Cells*. 2013;31(3):536-546.
20. Rothstein TL, Griffin DO, Holodick NE, Quach TD, Kaku H. Human B-1 cells take the stage. *Ann N Y Acad Sci*. 2013;1285:97-114.
21. Quách TD, Hopkins TJ, Holodick NE, et al. Human B-1 and B-2 B cells develop from Lin–CD34+CD38lo stem cells. *J Immunol*. 2016;197(10):3950-3958.
22. Sawai CM, Babovic S, Upadhaya S, et al. Hematopoietic stem cells are the major source of multilineage hematopoiesis in adult animals. *Immunity*. 2016;45(3):597-609.
23. Corat MA, Schlums H, Wu C, et al. Acquired somatic mutations in PNH reveal long-term maintenance of adaptive NK cells independent of HSPCs. *Blood*. 2017;129(14):1940-1946.

DOI 10.1182/blood.2019001343

2019 134: 89-92
doi:10.1182/blood.2019001343 originally published online May 21, 2019

A population of CD20^{+}CD27^{+}CD43^{+}CD38$^{lo/int}$ B1 cells in PNH are missing GPI-anchored proteins and harbor *PIGA* mutations

Yuki Kageyama, Hiroshi Miwa, Isao Tawara, Kohshi Ohishi, Masahiro Masuya and Naoyuki Katayama

Blood (print ISSN 0006-4971, online ISSN 1528-0020), is published weekly by the American Society of Hematology, 2021 L St, NW, Suite 900, Washington DC 20036.

Supplementary information

A population of $CD20^+CD27^+CD43^+CD38^{lo/int}$ B1 cells in PNH are missing GPI-anchored proteins and harbor *PIGA* mutations

Kageyama et al.

Supplementary Materials and Methods

Cell isolation

For sample collection, 10–20 mL of heparinized blood was drawn from each PNH patient. PB total nucleated cells and mononuclear cells were isolated by HetaSep (STEMCELL Technologies, Vancouver, BC, Canada) and density gradient centrifugation using Ficoll-Paque Plus (GE Healthcare Life Sciences, Uppsala, Sweden), respectively. $CD19^+$ cells were purified using a CD19 Microbeads kit (Miltenyi Biotec, Bergisch Gladbach, Germany). The processed cells were stored at 4°C and analyzed within 24 hours or suspended in CellBanker 1 (Nippon Zenyaku Kogyo, Koriyama, Japan) and stored in liquid nitrogen until analysis.

Flow cytometry and cell sorting

Isolated PB cells ($1–5 \times 10^6$/sample) in fluorescence-activated cell sorting buffer (phosphate-buffered saline with 2% fetal bovine serum and 1 mM EDTA) were incubated with Human TruStain FcX (BioLegend, San Diego, CA) for 10 minutes at room temperature to block Fc receptor binding and then stained with optimized concentrations of fluorochrome-conjugated monoclonal antibodies (mAbs) against CD3, CD11b, CD19, CD20, CD27, CD33, CD38, CD43, CD45, CD56, IgM, and IgD (mAb clones and sources are provided in supplemental Table 1) or isotype-matched control mAbs for 30 minutes on ice in the dark. FLAER was used to detect GPI-AP-deficient cells. Isolated PB cells were stained with FLAER under the same conditions used for mAbs. Dead cells were excluded by staining with 0.5 μg/mL 7-aminoactinomycin D (7-AAD) (BioLegend, San Diego, CA) for 5 minutes at room temperature in the dark. Samples were analyzed and sorted on BD LSRFortessa and BD FACSAria II (BD Biosciences, Franklin Lakes, NJ). To analyze B cell subpopulations, lymphocytes were gated by FSC and SSC. Doublets were excluded based on FSC-A and FSC-H. Dead cells and T cells were excluded by gating $7\text{-}AAD^-/CD3^-$ cells. $CD20^-CD38^{high}$ plasmablasts were excluded by gating $CD20^+$ cells. $CD20^+CD38^{high}$ pre-plasmablasts (or plasmablast precursors) were excluded by gating $CD38^{lo/int}$ cells. B cell subpopulations (B1 cells, naïve B cells, and memory B cells) were individualized and sorted on the basis of CD27 and CD43 expression (Figure 1A). Granulocytes and monocytes were identified by CD45 and SSC. Doublets, dead cells, and T cells were excluded as with B cells. Granulocytes and monocytes were confirmed to be $CD11b^{hi}$ and $CD33^{hi}$, respectively. To analyze T cells and NK cells, lymphocytes were gated by FSC and SSC. Doublets and dead cells were excluded as with B cells. B

cells and myeloid cells were excluded by gating $CD19^-$ and $CD33^-$, respectively. T cells and NK cells were individualized as $CD3^+$ and $CD3^-CD56^+$, respectively. Fluorescence-minus-one controls were used to set the gates for CD27, CD38, CD43, IgM and IgD, and isotype-matched control mAbs were used for all other antigens. Post-sort analysis revealed a purity of > 95%. Data were analyzed using FlowJo software v. 10.4.1 (FlowJo, Ashland, OR).

Sanger sequencing

Genomic DNA was extracted from PB samples using a NucleoSpin Tissue kit (Macherey-Nagel, Düren, Germany) and measured by a Qubit 3.0 Fluorometer (Thermo Fisher Scientific, Waltham, MA). For nucleotide sequence analysis, exons of the *PIGA* coding region and part of the introns flanking the exon were amplified by PCR using One Taq Hot Start DNA polymerase (New England BioLabs, Ipswich, MA) and the primers listed in supplemental Table 2. PCR amplification was performed for 35 cycles (denaturation at 94°C for 30 seconds, annealing at 55°C for 30 seconds, and extension at 68°C for 1 minute). The amplified products were sequenced using the BigDye Terminator v3.1 Cycle Sequencing kit and an Applied Biosystems 3730 DNA analyzer (Thermo Fisher Scientific) with the same primers used for PCR.

Digital PCR analysis

The allelic frequencies of mutations in *PIGA* in genomic DNA from patients PNH01 and PNH02 were estimated by digital PCR. The TaqMan probes and primers used for digital PCR are listed in supplemental Table 2. The 12.765 digital array was used with 8 μL reaction mixtures comprising 3.4 μL sample, 0.4 μL 20× gene expression sample loading reagent (Fluidigm, South San Francisco, CA), 0.2 μL 40× custom TaqMan SNP genotyping assay (Thermo Fisher Scientific) and 4.0 μL TaqMan gene expression master mix (Thermo Fisher Scientific). Loaded arrays were transferred to the Biomark HD system (Fluidigm) and the reactions were conducted as follows: 2 minutes at 50°C and 10 minutes at 95°C, followed by 40 cycles of 15 seconds at 95°C and 1 minute at 60°C. Fluidigm Digital PCR Analysis Software v4.1.2 was used to analyze the data, with a manual determination of the fluorescence threshold.

Bacterial cloning analysis

Genomic DNA extracted from PB cells of patient PNH01 was amplified using PCR primers covering the two mutation sites (supplemental Table 2). PCR products were purified and inserted into T-vector pMD20 using Mighty TA-cloning Kit (TaKaRa Bio, Kusatsu, Japan), and the plasmid was transformed into *E. coli* DH5α-competent cells (TaKaRa Bio). The resulting colonies were picked, expanded, and screened for the correct insert. Colonies with the correct insert were expanded, and plasmid DNA was extracted and analyzed by nucleotide sequencing.

For original data, please contact n-kata@clin.medic.mie-u.ac.jp.

Supplementary data

Supplemental Table 1. Antibodies used for flow cytometry and cell sorting

Antigen	Clone	Fluorochrome	Source
CD3	OKT3	FITC, Brilliant Violet 510, PerCP-Cy5.5	BioLegend
CD11b	ICRF44	PE	BioLegend
CD19	HIB19	PE-Cy7, Brilliant Violet 421*	BioLegend
CD20	2H7	Brilliant Violet 510, Brilliant Violet 785*	BioLegend
CD27	L128	APC	BD Biosciences
CD33	P67.6	PerCP-Cy5.5, APC	BioLegend
CD38	HB-7	APC-Cy7	BioLegend
CD43	1G10	PE	BD Biosciences
CD45	2D1	Brilliant Violet 421	BioLegend
CD56	5.1H11	PE, Brilliant Violet 421	BioLegend
IgM	MHM-88	Brilliant Violet 650	BioLegend
IgD	IA6-2	Brilliant Violet 510	BioLegend

* Used for analysis of IgM and IgD expression.

Supplemental Table 2. Primers and probes used for Sanger sequencing and digital PCR analysis

Gene		Dye	Oligo sequence (5′ to 3′)
PIGA Exon 2-1	Forward	–	GTTTCTGAGCTGAGATCCTG
	Reverse	–	GAGCATCATGGGCCATAGCA
PIGA Exon 2-2	Forward	–	GTCATGTACAACCAGTCTAC
	Reverse	–	GCCAAACAATCATTATATACAAG
PIGA Exon 3	Forward	–	TGGATTCTCAGTCGTTCTGGTGA
	Reverse	–	ATGCAGGAGAAGCAACACAC
PIGA Exon 4	Forward	–	TCACTCCTTTCTTCCCCTCTC
	Reverse	–	AATCCCAACCATGAATGCCCTC
PIGA Exon 5	Forward	–	TCTTCCTGAGGTATGATTATGGTG
	Reverse	–	AAGAGTTCAGACACAATCTTTTCTC
PIGA Exon 6	Forward	–	GGTCATTGTTTATCATGGGACAG
	Reverse	–	TCTTACAATCTAGGCTTCCTTC
PIGA c.464C>T	Forward	–	CTTCCACGCCAAGACAATGG
	Reverse	–	GTAAGCACCGAGCTGACATCA
	Probe 1	VIC-MGB	ACGGACCATTCCCTTTT
	Probe 2	FAM-MGB	ACGGACCATTTCCTTTT
PIGA c.548G>A	Forward	–	GCTTCTAACCGTGTCTCTTTGTGAT
	Reverse	–	GATTCAGTGCTGCTCTTAGTACAGT
	Probe 1	VIC-MGB	CCACATCATTTGTGTGTCT
	Probe 2	FAM-MGB	ACCACATCATTTATGTGTCT
PIGA c.848+1G>A	Forward	–	GGAAGAAGTTCGGGAAAGATACCA
	Reverse	–	TTCTCCCTCAAGACAACATGAAATTCA
	Probe 1	VIC-MGB	CTGCATGACAGGTATTGA
	Probe 2	FAM-MGB	TGCATGACAGATATTGA

Supplemental Table 3. Percentages of FLAER^{-} cells in each cell population of PNH patients

	Granulocyte	Monocyte	B1 cell	Naïve B cell	Memory B cell	T cell	NK cell
PNH01 1st	97.0	97.2	4.40	10.2	0.04	38.4	84.8
PNH01 2nd[*]	97.8	97.2	2.20	2.73	0.09	53.4	92.5
PNH02 1st	99.9	100.0	6.00	8.62	0.39	18.7	33.7
PNH02 2nd[†]	96.3	99.9	4.66	15.6	1.74	37.7	32.5
PNH03 1st	68.5	94.0	8.39	37.0	0.91	1.40	44.3
PNH03 2nd[‡]	84.2	95.9	8.80	50.2	1.96	0.43	40.8
PNH04 1st	100.0	100.0	3.79	25.0	0.22	1.40	2.10
PNH05 1st	99.8	99.6	4.62	40.2	0.25	6.50	100.0
PNH06 1st	77.9	75.3	5.98	50.8	1.37	9.90	73.7

[*]After 24 months from 1st sampling.

[†]After 29 months from 1st sampling.

[‡]After 35 months from 1st sampling.

Supplemental Table 4. Ratio and absolute numbers of $CD19^+$ cells, B1 cells, and $FLAER^-$ B1 cells

	$CD19^+$ cells in WBC (%)	B1 cells in $CD19^+$ cells, (%)	No. of B1 cells ($\times 10^6$/L)	No. of $FLAER^-$ B1 cells ($\times 10^6$/L)
PNH01 1st	1.87	5.64	2.53	0.11
PNH01 2nd	0.81	4.41	2.03	0.04
PNH02 1st	3.91	3.88	5.82	0.34
PNH02 2nd	3.28	4.69	5.07	0.23
PNH03 1st	3.18	4.27	2.17	0.18
PNH03 2nd	3.75	4.26	2.39	0.21
PNH04 1st	4.80	4.64	14.03	0.53
PNH05 1st	5.92	6.63	14.52	0.66
PNH06 1st	1.87	12.90	13.41	0.80

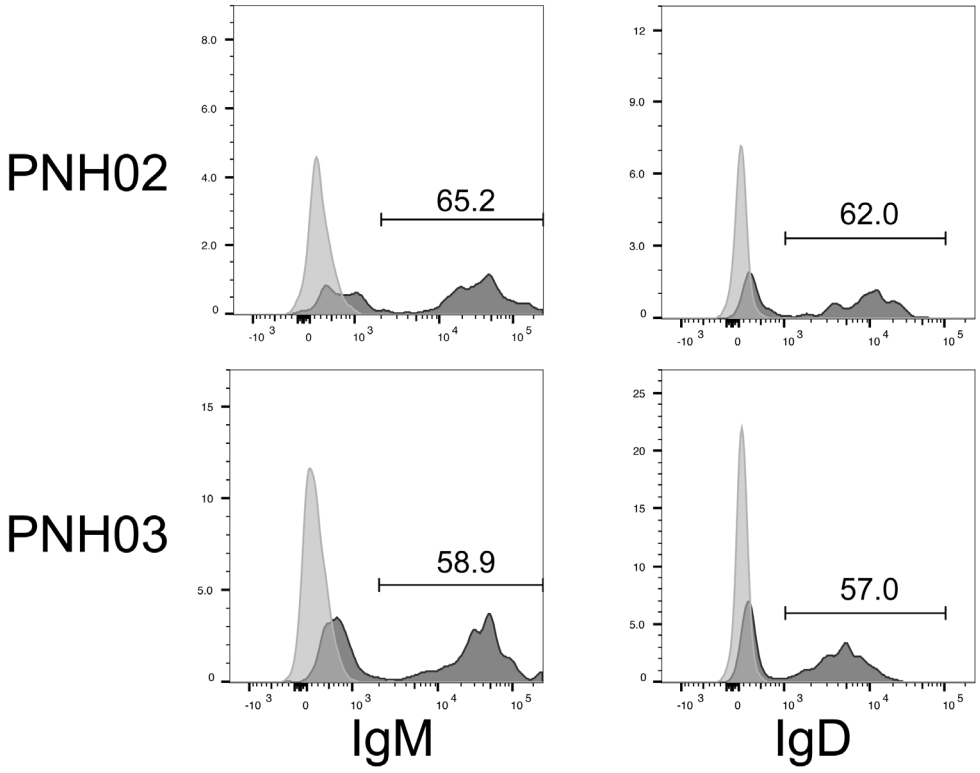

Supplemental Figure 1. IgM and IgD expression on FLAER^{-} B1 cells from patients PNH02 and PNH03. FLAER^{-}CD19^{+}CD20^{+}CD27^{+}CD43^{+}CD38$^{lo/int}$ B1 cells from the second samples were stained with anti-IgM and anti-IgD mAbs. Histograms of the fluorescence-minus-one controls are shown in light gray. The percentage of positive cells is indicated on each histogram.

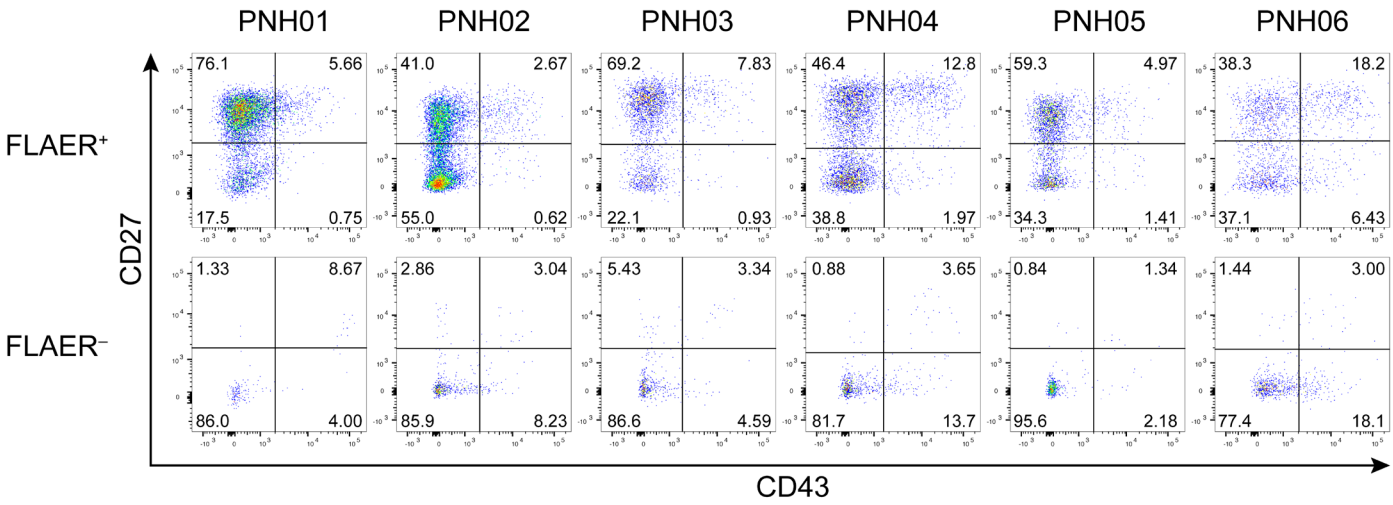

Supplemental Figure 2. B cell subpopulations in FLAER$^+$ and FLAER$^-$ cells. CD19$^+$CD20$^+$CD38$^{lo/int}$ cells from the first samples of all six patients were divided into FLAER$^+$ and FLAER$^-$ fractions. These fractions were then analyzed for expression of CD43 and CD27. The percentages of each cell subpopulation are indicated in the plot areas.